Journal of Cleaner Production 483 (2024) 144242

Contents lists available at ScienceDirect

Journal of Cleaner Production

journal homepage: www.elsevier.com/locate/jclepro

# Operational energy savings in greenhouses by retrofitting covering plastics with photothermal antimony tin oxide nanocoating

Mohammad Elmi [a], Enhe Zhang [a], Anwar Jahid [a], Julian Wang [a,b,*]

[a] Department of Architectural Engineering, The Pennsylvania State University, University Park, PA, 16802, USA
[b] Materials Research Institute, The Pennsylvania State University, University Park, PA, 16802, USA

ARTICLE INFO

Handling Editor: Jin-Kuk Kim

*Keywords:*
Energy saving
Greenhouse energy system
Photothermal
Plasmonic nanoparticles
Nanocoating
Controlled environment agriculture

ABSTRACT

Energy management in greenhouses is crucial as they demand high energy consumption to keep a desirable environment for products. In this study, a novel greenhouse covering coating is introduced based on photothermal plasmonic nanoparticles to reduce energy consumption in greenhouses. Antimony tin oxide nanoparticles were used as plasmonic nanoparticles and were deposited on polyethylene greenhouse coverings. Thermal and optical properties of the antimony tin oxide-coated covering were characterized, and a comprehensive seasonal greenhouse energy analysis was performed to investigate the energy performance of the developed greenhouse covering. The photosynthetically active radiation (PAR) transmittance of the developed covering is 0.746, and the PAR-to-Solar-Transmittance (PST) value increased about 75% by the new covering. Based on the results, developed greenhouse covering with photothermal plasmonic nanoparticles drops greenhouse heating load by 70% and reduces total greenhouse energy consumption up to 49% in very cold climates. Antimony Tin Oxide nanocoating itself increases greenhouse energy saving by 11.4% in comparison with uncoated-double-layer polyethylene covering. Greenhouse energy savings in this study were achieved without any compromise in photosynthetically active radiation (PAR) and crop growth. A greenhouse covering utilization guideline is provided for each climate zone based on the results of this study to optimize the energy use in the greenhouse. This study opens a new window to innovative material applications in greenhouses to make greenhouses more sustainable and energy-efficient.

## 1. Introduction

One of the most basic human needs, food, has become more problematic as the world's population grows. Because of the human need for food, out-of-season cultivating has become commonplace and proven necessary, which has sped up the development of greenhouses (Chaysaz et al., 2019). Crops can be grown in a controlled atmosphere using greenhouse farming, which promotes quicker growth and better yields (Rabbi et al., 2019). A workable solution to guaranteeing wholesome food for an expanding human population is the sustainable cultivation of vegetables and fruits in greenhouses (Nikolaou et al., 2021). The production of agricultural commodities, on the other hand, is largely responsible for the world's human-induced greenhouse gas emissions (Muñoz-Liesa et al., 2022). According to estimates from the UN Food and Agriculture Organization, land use-related and agriculture emissions are responsible for approximately 17% of overall worldwide greenhouse gas emissions. Thus, the agriculture industry has a significant impact on climate change and global warming (Brækken et al., 2023).

Crop growth depends on the interior microclimate, specifically the greenhouse's thermal management (Liu et al., 2023). Nevertheless, maintaining a comfortable environment in the greenhouse, particularly when cultivating crops in the off-season, requires high energy consumption (Al-Helal and Abdel-Ghany, 2011). As a result, expanding protected horticulture in greenhouses to boost output per unit area would result in higher energy use and associated environmental effects (Hosseini et al., 2024). Furthermore, this extensive energy use means significant energy expenses. Heating and cooling systems are among the major greenhouse operational expenses (Hosseini-Fashami et al., 2019). In certain situations, the total energy consumption might make up as much as 50% of the total costs of running a greenhouse. These high operational expenses due to high energy use negatively impact the profitability of the greenhouses (Brækken et al., 2023). Thus, energy-efficient greenhouse operation is critical, and there is an urgent

* Corresponding author. Department of Architectural Engineering, The Pennsylvania State University, University Park, PA, 16802, USA.
*E-mail address:* julian.wang@psu.edu (J. Wang).

https://doi.org/10.1016/j.jclepro.2024.144242
Received 9 September 2024; Received in revised form 12 November 2024; Accepted 14 November 2024
Available online 19 November 2024

need to switch to more environmentally friendly and greener technology in greenhouses.

Incorporating energy-efficient systems and sustainable energy solutions in greenhouses can make them more environmentally friendly and lower their energy consumption and energy costs (Hooshmandzade et al., 2021). Recently, researchers have started studying methods to lower greenhouse energy consumption by utilizing innovative tools and techniques.

Given the importance of the greenhouse's covering system to the heat exchange between the internal and external environment, covering materials play a vital role in energy management in greenhouses and have garnered a lot of attention. Ma et al. (2022) designed a novel greenhouse covering structure termed the spectral splitting covering, which was able to transmit photosynthesis-required light and convert the NIR light to electricity. They performed numerical simulations and provided greenhouse energy analysis based on their results. The visible transmissivity of their designed greenhouse covering was above 40% all day and the electric power of the covering reached 133.2 W/m$^2$. Feng et al. (2024) proposed a beam-splitting greenhouse covering to decrease the interior temperature and cooling energy consumption of the greenhouses in summer. They designed a greenhouse covering structure to transmit visible light and absorb the NIR light based on the spacing prism principle. They compared their results with a double-layer vacuum glass greenhouse covering and reported a greenhouse inside temperature reduction of 3.16 °C, which led to a 21% thermal load decrease by utilizing their designed covering. However, the impact of the proposed covering on the greenhouse total energy use and plant growth was not presented. Chen et al. (2020) analyzed phase change materials (PCMs) usage in plastic greenhouse coverings. They experimentally confirmed that using phase change materials can increase the greenhouse indoor temperature, but the energy savings analysis and the effect of PCMs on plant growth were not studied.

Numerous studies have been conducted on novel greenhouse covering coatings to enhance greenhouse energy efficiency. Low-E and IR-reflective coatings such as zinc oxide (ZnO) and titanium dioxide ($TiO_2$) have been studied in several researches. These coatings have high reflection in infrared and near-infrared (IR-NIR) regions which are important causes of heat accumulation in greenhouses. By using these coatings, it is possible to lower the surface temperatures of the covering materials in greenhouses by around 15%–20%, which would improve the environment for the growth of plants (Zhang et al., 2023). Nevertheless, utilizing these coatings typically has a negative impact on the solar heat gains in winter as they decrease the Solar Heat Gain Coefficient (SHGC) of the greenhouse covering. On the other hand, using Low-E or IR-reflective coatings is mostly accompanied by significant visible transmittance reduction and results in lowering the greenhouse's productivity (Abdel-Ghany et al., 2012). Therefore, even though these technologies effectively handle the overheating problem, they offer a crucial trade-off by affecting the greenhouse's light environment. Additionally, previous research has suggested that the lower surface temperatures caused by the use of Low-E coatings might also mitigate the condensation resistance of the covering materials, especially under high humidity conditions of greenhouses (Zhang et al., 2023). This, in turn, could lead to an increase in energy consumption due to the formation of condensation on the inner surfaces. Also, there is still a huge lack of technology to deposit Low-E coatings on plastics. The intrinsic characteristics of plastics, such as their low surface energy and flexibility, make it difficult for Low-E materials to be effectively deposited on plastics, compromising the durability and overall performance of Low-E coated covering materials in greenhouses (Solovyev et al., 2015). Xie et al. (2019) studied indium tin oxide/silver (ITO/Ag) composites to enhance the optical properties of the greenhouse covering. They executed numerical calculations and reported more than 95% visible light transmittance and more than 90% NIR reflectance. Although the optical features of the greenhouse are perfectly improved, there is still a lack of detailed energy analysis to show how these coatings change the total energy use of the greenhouse. In the other work by Chavan et al. (2020), a smart glass film (ULR-80) was employed on greenhouse covering to reduce greenhouse energy use. They studied the optical properties of the structured covering and energy savings in the greenhouse. Based on their results, 85 % of the ultraviolet (UV), 26% of red and 58% of far-red light were blocked. As a result, the heat load was reduced by 8%. In contrast, utilizing these films led a 19% reduction in PAR and consequently 25% decrease in season fruit production. Solovyev et al. (2015) worked on multilayer low-E coatings on polyethylene terephthalate (PET) and polyethylene (PE) substrates. They optimized low-E coatings' structures experimentally and used ZnO:Ga/Ag/ZnO:Ga/$SiO_2$ films as the coating on the PE greenhouse coverings. They reported 77% transmittance and 91–92% IR reflection of their developed coating. They performed heat transfer calculations and reported that the greenhouse energy consumption decreased to the half in one day in winter utilizing developed coating. In addition to the complexity of the coating structure, lack of comprehensive greenhouse energy analysis with and without coating is observed in this research work.

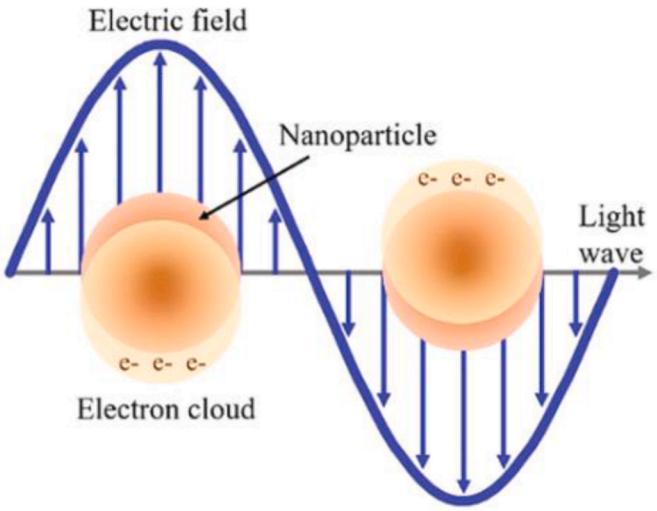


**Fig. 1.** The schematic of LSPR.

Considering the limitations associated with traditional coatings on greenhouses' covering materials, new studies on innovative coating materials are needed in order to reduce the yearly total greenhouse energy use without sacrificing the light needed for photosynthesis and crop growth. In addition, coatings should be compatible with common greenhouse coverings and easy to coat and use. Also, the literature review revealed that there is a lack of comprehensive energy studies of greenhouses with energy-efficient coverings that simultaneously consider the effects on PAR and crop growth. Furthermore, the impacts of different climate conditions on the energy efficiency of these coverings are barely studied. The novelty of this work is to introduce a new greenhouse covering coating material based on the photothermal energy conversion and intrinsic plasmonic nanoparticles features. By leveraging photothermal principles, these coatings have the potential to achieve optimal energy use while minimizing the drawbacks and complications of traditional coatings. A comprehensive annual, monthly, and daily greenhouse energy analysis is performed across eight different climate zones. The effects on PAR and crop growth are investigated. The energy performance of the developed greenhouse covering is then compared to that of traditional greenhouse coverings.

### 1.1. Photothermal plasmonic nanoparticles

Photothermal conversion or light-to-heat conversion is the process in which the light's energy is transferred to heat through light-absorbing materials. High-performing photothermal materials are highly capable

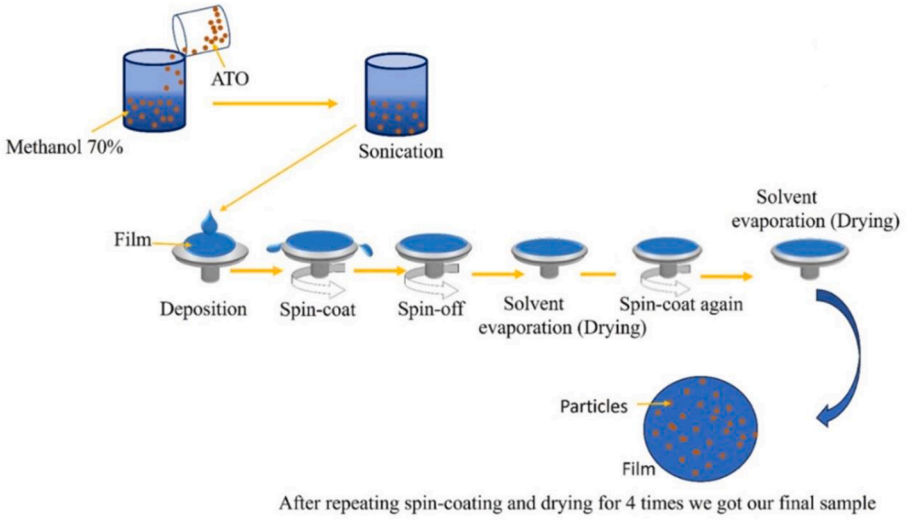


**Fig. 2.** The schematic of the ATO nanoparticles coating process.

of absorbing light and efficiently converting light into heat (Cui et al., 2023). Various materials have different photothermal mechanisms based on their electronic structures (Elmi and Wang, 2023).

The photothermal mechanism which takes place in plasmonic nanoparticles is plasmonic localized heating. Localized surface plasmon resonance (LSPR) occurs when the incoming light's frequency aligns with the natural frequency of the plasmonic nanoparticles' electrons which causes oscillations of free electrons. As a result of the generation and relaxation of hot electrons, heat is generated and then the heat is transferred to the surrounding medium (Chen et al., 2019). The schematic of the LSPR is shown in Fig. 1.

Also, plasmonic nanoparticles can be spectrally selective, which allows us to adjust the absorption spectrum of the coating to transmit the essential light spectrum for photosynthesis and absorb the NIR light. The oscillations of the free electrons caused by LSPR lead to a strong enhancement of the electric field close to the surface, and the material's absorption at corresponding wavelengths increases significantly. This peculiar behavior of plasmonic nanoparticles is linked to their special electronic configurations, in which electrons coherently oscillate and redistribute on the surface. Plasmonic nanoparticles respond to light depending on their morphology, shape, size, shape, and surrounding medium (Indhu et al., 2023). Therefore, the absorption spectrum of the plasmonic nanoparticles can be finely tuned by some of their properties like shape and size. As discussed, instead of reflecting NIR, photothermal materials absorb near-infrared light. It means that in addition to preventing NIR light from passing through the covering, photothermal coatings do not reduce the SHGC of the covering as much as other coatings do, and help greenhouse coverings to keep their high SHGC value. As a result, they do not affect thermal control negatively in winter. Also, these nanoparticles are easy to deposit on plastics such as Polyethylene (PE), Which is the most common plastic used in greenhouses (Katsoulas et al., 2020). This research uses enhanced photothermal characteristics of plasmonic nanomaterials such as surface plasmon resonance to decrease energy consumption in greenhouses and present novel greenhouse coating materials to make greenhouses more energy-efficient and sustainable.

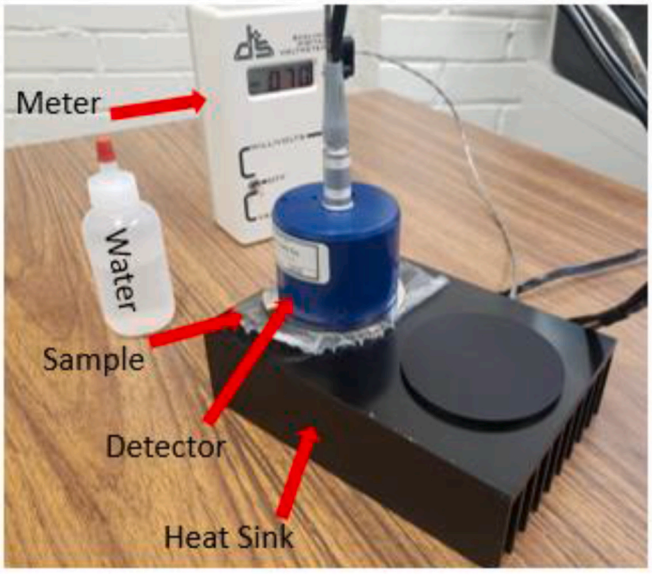


**Fig. 3.** The experimental setup to measure samples' emissivity.

## 2. Materials and methods

### 2.1. Materials and coating

Polyethylene (PE) is used as a greenhouse covering material in this study. Because of its durability and resistance in extreme weather conditions, PE is commonly used as a covering material in greenhouses. Although PE is so light with a density of about half of the glass, it has impressive flexibility and rigidity, which make it suitable to be used in greenhouses. PE substrates were purchased from Farm Plastic Supply (Addison, IL, USA) and were used as received. Antimony Tin Oxide (ATO) nanoparticles with an average particle size between 20 and 50 nm and a purity of 99.5% were purchased from Thermo Fisher Scientific Chemicals Inc. (Tewksbury, MA, USA) as powder.

A measure of 5g ATO nanopowder was poured into 100 ml of 70% methanol solution, followed by 60 min sonication to make the solution homogeneous. Then $10 \times 10$ $cm^2$ PE substrates were spin-coated by ATO nanoparticle solution using 80 μL solution per spin-coating time. The spin time and speed were 30 s and 1000 rpm, respectively. To achieve more ATO nanoparticles on a substrate, 4 layers of ATO were deposited on a sample. To this end, after the first coat, the sample was dried for 2 h at room temperature, and then the second spin-coating was applied to the sample. This procedure was repeated 4 times to obtain a 4-ATO-layer-coated sample denoted as PE-ATO4. The schematic of the coating process is depicted in Fig. 2.

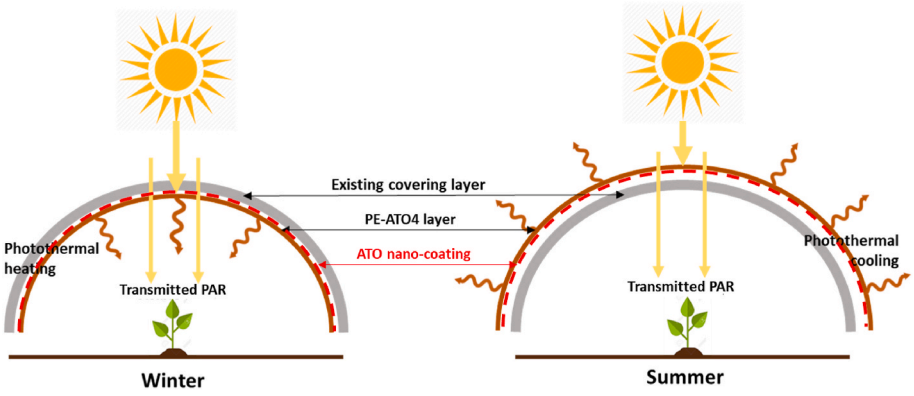


**Fig. 4.** The schematic of the seasonal setup of ATO-coated PE films.

### 2.2. Characterization methods

#### 2.2.1. Deposition characterization

To investigate the ATO nanoparticles deposition on PE samples and study coating quality, scanning electron microscopy (SEM, Thermo Scientific Apreo 2 SEM), X-ray photoelectron spectroscopy (XPS), and X-ray diffraction (XRD) were taken. XPS measurements were conducted using Physical Electronics VersaProbe III (Al kα) covering approximately 200 μm diameter. All spectra were calibrated with reference to the C1 peak at 284.8 eV. XRD patterns were measured by Malvern Panalytical Empyrean® with copper Kα radiation ($\lambda = 1.5406$ Å) at 45 kV and 40 mA within diffraction angle $2\theta$ from 10° to 70°. The scanning step size was 0.02°.

#### 2.2.2. Optical characterization

Optical characterization includes determining transmittance, reflectance, and the emissivity of the samples. Optical spectra were obtained by Cary 5000 UV–Vis–NIR spectrometer with a 150 mm integrating sphere. The spectral range was 300–2000 nm with a step size of 1 nm. The emissivity was measured by the process described in our previous work using the AE-AD1 emissometer (Zhang et al., 2023). The experimental setup for measuring the emissivity of samples is demonstrated in Fig. 3. The optical characterization was performed for both PE and PE-ATO4 samples.

#### 2.2.3. Thermal characterization

The primary thermal properties in this study are the center-of-the-covering U-factor and Solar Heat Gain Coefficient (SHGC). These properties were determined following ISO 15099 and National Fenestration Rating Council (NFRC) standards using LBNL WINDOW Software and its OPTICS by optical characterization data (Curcija et al., 2015). To comprehensively study the impact and potential energy savings of the developed ATO-coated PE plastics on the greenhouse's energy consumption, three different greenhouse coverings were modeled.

- **Single-Layer PE Film**: The foundational covering is a single-layer polyethylene (PE) film, 6-mil (approximately 0.15 mm) thick. This material is favored in numerous climates for its straightforward installation, affordability, and high solar transmittance, making it a prevalent choice for greenhouse construction.
- **Double-Layer PE Covering**: The next variant explored is a double-layer PE covering, consisting of two 6-mil PE layers separated by a 13 mm air gap. Recently introduced to greenhouse insulation techniques, this configuration aims to enhance insulating properties, thereby extending the growing season. It can be implemented as either an initial installation in new constructions or, more often, as an upgrade by adding a second layer to an existing single-layer setup of greenhouses.
- **PE-ATO4 Covering**: The third and new covering examined in this research is based on the double-layer model but incorporates one 6-mil PE layer and one 6-mil ATO-coated PE (PE-ATO4) layer, maintaining the same 13 mm air gap. The inclusion of a nanocoated layer (PE-ATO4) necessitates careful consideration of its orientation during installation—external or internal—to leverage its thermal management benefits effectively. Our investigation includes a seasonal adjustment strategy for this coated layer to examine its impact on operational energy efficiency. In the summer, aiming for reduced solar heat gains, the coated layer is placed externally (surface 2; outer surface facing outdoors is typically defined as surface 1) to dissipate the absorbed solar infrared outward. Conversely, in winter, the layer is installed internally (surface 3) to maximize heat retention inward. This seasonal switch design is illustrated in Fig. 4. Summer and winter seasons are defined differently for the various climatic zones, which is determined based on our previous work (Anwar Jahid et al., 2022). This is further discussed in the Results and Discussion section. Notably, the proposed seasonal switch paradigm presented in this work is practical and aligns with common greenhouse energy-saving practices. It builds on the widespread method of adding or installing new layers or materials to existing coverings to

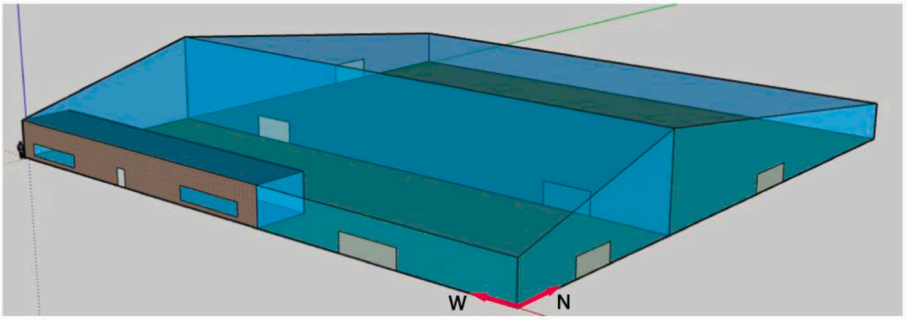


**Fig. 5.** The greenhouse model used in this study.

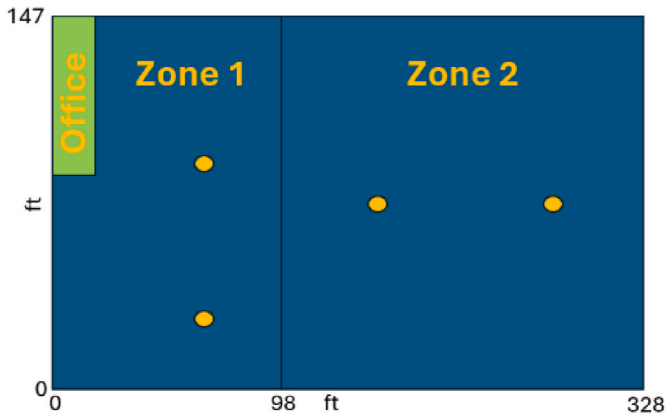


**Fig. 6.** Illuminance setpoints.

enhance thermal efficiency across various climates, such as the installation of dark shade cloth within greenhouses during summer or augmenting insulation with an additional plastic layer in winter.

Given the optical properties of the PE and PE-ATO4 samples derived from OPTICS of the LBNL WINDOW software and optical characterization data, the center-of-the-covering U-factor and the covering's Solar Heat Gain Coefficient (SHGC) are calculated. In U-factor calculations, based on mentioned standards, the interior and exterior ambient temperatures are assumed as 21, and -18 °C. The wind speed is set to 5.5 m/s.

### 2.3. Energy model

A greenhouse energy model was developed and simulated in EnergyPlus. The greenhouse model was developed using the DOE Prototype Building Model, Warehouse (non-refrigerated) ASHRAE 90.1 2019, with some modifications to meet greenhouse standards (Baglivo et al., 2020; Choab et al., 2021; Pacific Northwest National Laboratory (PNNL), 2023). Fig. 5 shows the greenhouse model in EnergyPlus. All exterior walls and the roof of the prototype model were changed to window glazing with a 30° slope of the roof. The total area of the modeled greenhouse is 52,045 $ft^2$, and all dimensions were kept as prototype building models by DOE.

#### 2.3.1. HVAC settings

The HVAC system parameters in the model were adjusted as described below (Jans-Singh et al., 2021).

- **Heating:** The heating setpoint was set to 16 °C for 6 a.m. to 9 p.m. and 13.6 °C for other times. The heating was provided by natural gas using heating coils, and the heating supply air temperature was set to 50 °C.
- **Cooling:** The cooling setpoint was adjusted to 27 °C for 6 a.m. to 8 p.m. and 29.7 °C for other times of the day. The air-cooled condenser was employed to provide cooling using electricity with a supply cooling air temperature of 14 °C.

The fan system energy consumption was minimized by assuming the design pressure rise as 240 Pa.

#### 2.3.2. Lighting settings

Different greenhouse plants require varying photosynthesis light quality and intensity, which can also vary throughout different growth stages. However, for the purpose of accurately and fairly assessing the impact of covering materials on operational energy use, we simplified the lighting requirements, following established practices in previous greenhouse energy studies (Gislerød et al., 2012; Iddio et al., 2020; Ravishankar et al., 2022; Xu et al., 2020). According to current literature, the recommended minimum PPFD ranges from 200 to 360 μmol/$m^2$s for greenhouse leafy vegetables such as lettuce, basil, and tomatoes (Ke et al., 2021). To avoid underestimating the lighting energy use and the impact of transmitted solar light affected by the covering materials, we opted to utilize the higher recommended PPFD value of 360 μmol/$m^2$s.

Since EnergyPlus does not directly incorporate PPFD for lighting automation, we converted the PPFD value to the photopic lux value of 19,440 lux as a setpoint in lighting automation systems of EnergyPlus. In particular, the lighting system in EnergyPlus was programmed to operate for 16 h daily to meet the minimum lighting requirement, with an automatic shutdown for the remaining 8 h at night. Automated lighting controls were implemented with continuous offsetting and set to maintain a minimum input power and light output fraction of 0.2. The illuminance reference points were strategically placed to control greenhouse zones 1 and 2 (yellow points), as illustrated in Fig. 6. These control settings help the greenhouse to maintain (turned on with dimming if needed) sufficient light quality for plant growth during daytime and turned off during nighttime. Additionally, to consider the potential heat emitted from the lights, 31% convective and 17% radiative heat dissipation were defined in EnergyPlus based on prior studies (Katzin et al., 2021).

The variable parameters in the EnegyPlus model are U-factor, SHGC, and PAR transmittance of each covering sample derived from LBNL Window software. After the model was entirely developed, the EnergyPlus simulation was executed, and heating, cooling, lighting, and total energy consumption results were obtained. To comprehensively investigate the effects of photothermal coatings on greenhouse energy consumption, a simulation was executed for eight different US climate zones, and results are compared and discussed.

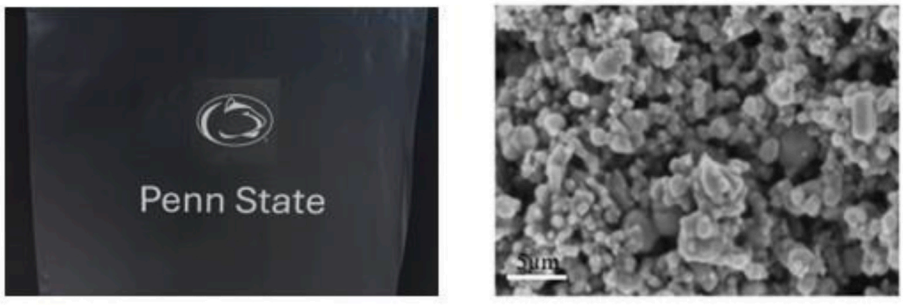


**Fig. 7.** (a) The ATO-deposited PE sample (b) SEM image of ATO nanoparticles (scale bar is 5 μm).

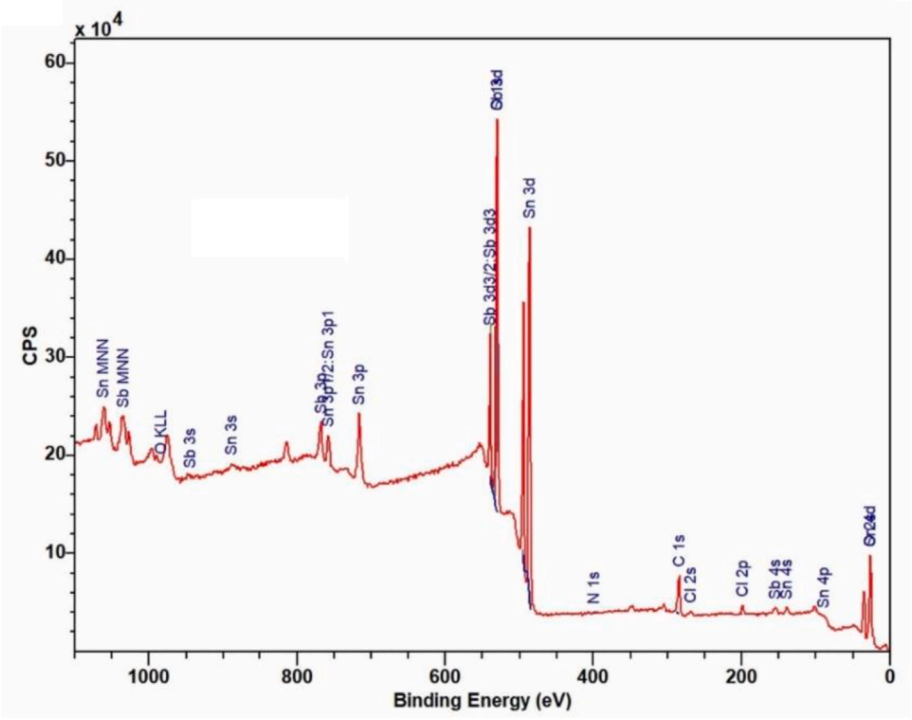


**Fig. 8.** Total XPS spectra of ATO-coated PE.

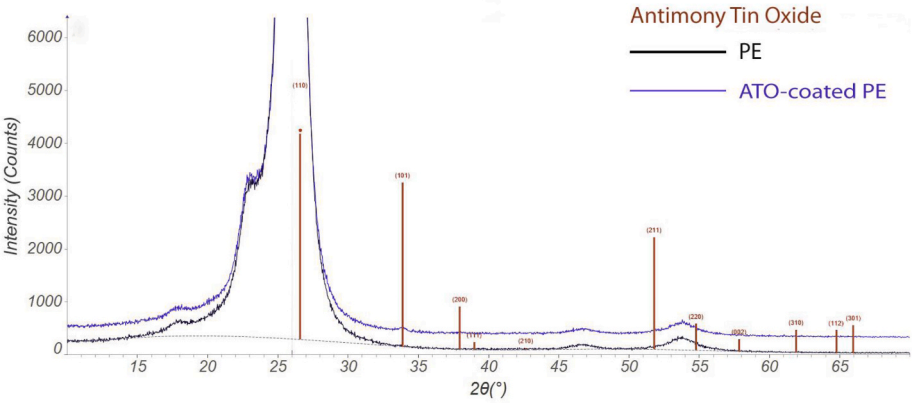


**Fig. 9.** XRD pattern of PE and ATO-coated PE.

## 3. Results and Discussion

### 3.1. ATO nanoparticles deposition

The ATO deposition quality on the PE surface is investigated by various characterization techniques. Fig. 7 shows the PE sample after ATO deposition and the SEM image of the coated sample. ATO nanoparticles are clearly shown on the SEM image, which proves their existence on the surface. An in-depth understanding of the surface chemistry and stability of the ATO nanoparticle coatings on the PE substrate was provided by the XPS and XRD analysis. As presented in Fig. 8, the XPS results validate the antimony presence on PE samples, showing effective ATO nanoparticles coating on PE. The components' identification aligns with the anticipated chemical composition of the film surfaces after nanoparticle deposition.

Fig. 9 provides XRD patterns of coated PE. The bare PE has a distinct peak at approximately 28° 2$\theta$, which is characteristic of its amorphous structure, where the peak at 33.9° 2$\theta$ matches the tetragonal ATO (101), showing that the ATO nanoparticles are present on the sample. The XRD results of tetragonal ATO crystallinity are consistent with antimony detection of XPS analysis. The XPS and XRD results verify that the ATO nanoparticles are uniformly deposited on the PE substrates.

**Table 1**
Emissivity values.

| Sample | Emissivity |
|---|---|
| PE | 0.86 |
| PE-ATO1 | 0.71 |
| PE-ATO4 | 0.42 |

### 3.2. Optical and thermal properties

Optical properties of the samples are vital in this study as aims to selectively filter the solar radiation while minimizing the compromise in required photosynthesis light. Therefore, UV–Vis–NIR spectra and PAR transmittance results should be thoroughly studied. In addition, surface

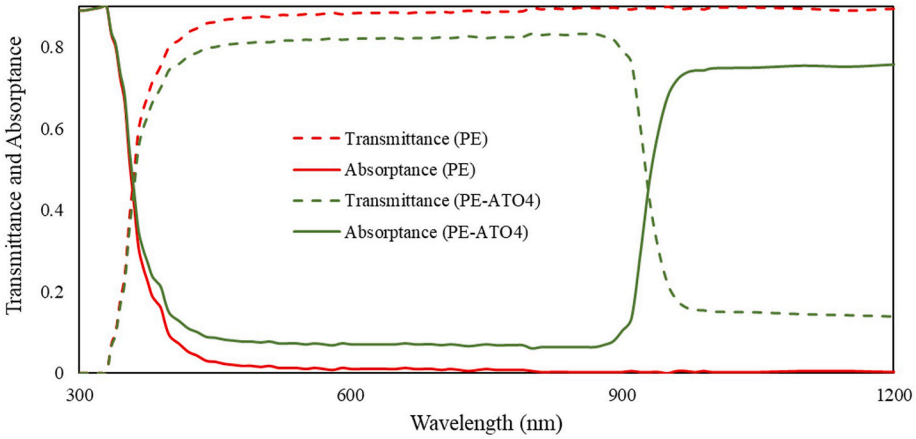


**Fig. 10.** The UV–Vis–NIR spectra of the PE and the PE-ATO4.

**Table 2**
PAR transmittance values of different greenhouse coverings.

| Covering | PAR Transmittance |
|---|---|
| Single-layer PE | 0.890 |
| Double-layer PE | 0.802 |
| PE-ATO4 | 0.746 |

**Table 3**
Thermal properties of the greenhouse coverings.

| Covering | U-factor (W/m$^2$K) | SHGC |
|---|---|---|
| Single-layer PE | 6.065 | 0.892 |
| Double-layer PE | 2.816 | 0.806 |
| PE-ATO4 (Summer) | 2.336 | 0.579 |
| PE-ATO4 (Winter) | 2.336 | 0.727 |

emissivity is important to study as affects the heating and cooling energy performance and it has a direct impact on the overall thermal insulating abilities of the covering material. The measured total emissivity values of the PE, one-layer-ATO-coated PE (PE-ATO1), and four-layer-ATO-coated PE (PE-ATO4) are provided in Table 1. It shows that the emissivity of the PE sample is diminished by the ATO coating. The intrinsic characteristics of the ATO nanoparticles, which are metallic in nature and have a low emissivity, may be the cause of this decrease. Also, as is indicated in Table 1, adding more ATO layers achieved a further decrease in the emissivity of the sample, which made it less than half ultimately by adding four layers, from 0.86 to 0.42. This decrease in emissivity could help in the covering's total heat transfer coefficient (U-factor) reduction, increasing the overall insulation of the covering, and consequently, saving heating and cooling energy in both winter and summer seasons. As is depicted in Table 3, the U-factor decreased from 2.816 to 2.336 W/m$^2$K due to the emissivity reduction by the added ATO coatings.

The optical spectra of the samples (PE and PE-ATO4) are depicted in Fig. 10. The bare PE is almost fully transparent in both PAR and NIR regions from 380 to 2000 nm. Almost no absorption occurs in PE samples in PAR and NIR regions. However, the absorptance of the PE-ATO4 begins to increase from the end of the PAR region (~860 nm) and it rapidly goes up more than 0.7 from the wavelength of 960 nm and maintains this high value in NIR. The PAR transmittance values of the different coverings are mentioned in Table 2. As is shown in Table 2 and Fig. 10, the transparency of the PE in the PAR range did not change a lot as a result of ATO coating. The total PAR transmittance of single-layer PE and PE-ATO4 are 0.890 and 0.746, respectively. It shows that although the absorption of PE is increased extensively in the NIR region by ATO coating, the transparency in the PAR region has just decreased by 0.144 in total. This is the distinctive characteristic of the plasmonic nanoparticles which is applied to PE samples by ATO coating. The NIR light is absorbed by ATO nanoparticles and filtered through the PE-ATO4 sample, while the PAR light, which is required for photosynthesis, is transmitted.

The center-of-the-covering U-factor and solar heat gain coefficient (SHGC) of the covering are the two most important thermal parameters of greenhouse coverings in thermal and energy calculations and management. Table 3 shows the calculated values of these parameters for different coverings. As anticipated, the double-layer PE has a much lower U-factor than the single-layer PE. It is mostly because of the 13 mm air gap, which creates a strong insulation and decreases the heat transfer. Also, there is a little drop in SHGC as the transparency of the double-layer PE is slightly reduced. The U-factor in PE-ATO4 is even less than double-layer PE. It is because of the less emissivity of the coated PE than bare PE.

The SHGC of the greenhouse covering is expressed as the difference between heat fluxes entering the greenhouse with and without incident solar radiation and is calculated using Equation (1).

$$SHGC = \tau_s + \frac{q_{in(IS=0)} - q_{in}}{I_S} \quad (1)$$

Where $\tau_s$ is the covering total solar transmittance, $q_{in}$ and $q_{in(IS=0)}$ are the heat fluxes entering the greenhouse with and without incident solar radiation, respectively. $I_S$ is the solar radiation rate per square meter (W/m$^2$) reached by the greenhouse. The term $q_{in(IS=0)} - q_{in}$ in Equation (1) is directly related to the covering absorptance. When light strikes the covering, part of it is transmitted inside, which directly contributes to solar heat gain. Some part of it is reflected with no effect on SHGC, and the other portion of the light is absorbed by the covering. Depending on which side of the covering the absorption occurs, the absorbed energy may be reradiated inside or outside of the greenhouse, which alters the inward heat-flowing fraction of SHGC. That's why the SHGC has different values in summer and winter conditions in this study. In summer, the coating layer is placed at the outside of the greenhouse (Fig. 4), and the absorbed energy by the coating is mostly reradiated to the outside, and a small amount of it contributes to the SHGC. On the other hand, in winter, when the coating layer is internal, the absorbed energy is mostly reradiated and enters the inside of the greenhouse. Thus, the SHGC of PE-ATO4 is greater in winter than in summer. This difference helps in energy management in the greenhouse as more natural heat is required in winter and less solar heat entering the greenhouse reduces cooling energy in summer. This is the reason that traditional coatings such as Low-E coatings reversely affect SHGC and thermal management. As traditional coatings have high reflectance in

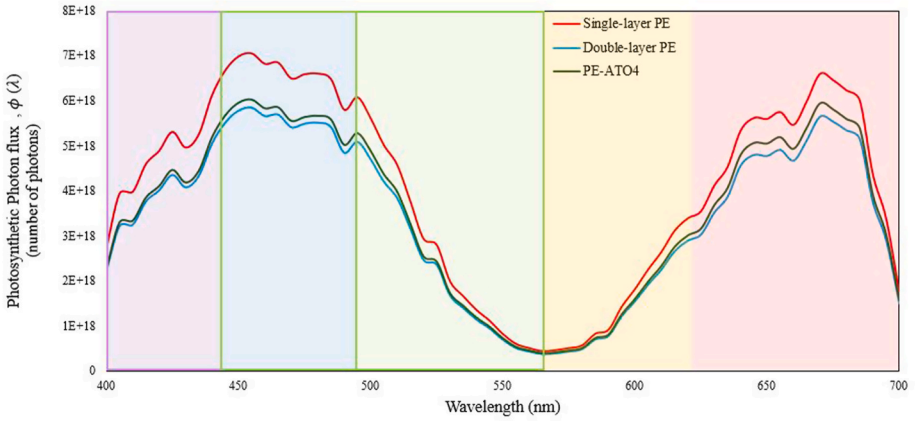


**Fig. 11.** Photosynthetic photon flux, $\varphi$ ($\lambda$), for different greenhouse coverings.

the NIR region, they cause the SHGC of the coated covering significantly decreases. Therefore, solar heat is being prevented from entering the greenhouse in winter. This is one of the main advantages of plasmonic nanoparticles rather than traditional coatings on greenhouse coverings. As plasmonic nanoparticles have high absorption, rather than reflection, in the NIR region, they help coverings maintain high SHGC during winter, which helps in energy saving in the greenhouse. Here, although the NIR transparency of the PE-ATO4 is much less than single and double-layer PE, because of the high absorption capacity of ATO nanoparticles, the SHGC of the PE-ATO4 covering is only about 10% less than double-layer PE in winter, and about 25% less in summer, which is beneficial in thermal and energy management.

### 3.3. Effects on photosynthetically active radiation (PAR) and plants growth

#### 3.3.1. Photosynthetic Photon Flux Density (PPFD)

Photosynthetic Photon Flux Density (PPFD) is a crucial metric representing the quantity of photosynthetically active photons that reach a specific area within a given timeframe. PPFD is measured in micromoles per square meter per second (μmol/$m^2$s). This metric provides valuable insights into the intensity of light available for photosynthesis, which is the process through which plants convert light energy into chemical energy to fuel their growth and development. For plants, light is an essential factor influencing various physiological processes, including photosynthesis, photomorphogenesis, and photoperiodism. PPFD specifically quantifies the number of photons in the photosynthetically active range (typically 400–700 nm) that reach the plant canopy. The intensity of PPFD directly impacts the rate of photosynthesis; an optimal PPFD ensures that plants receive sufficient light energy to carry out this crucial process efficiently. Studies showed that there is a positive correlation between increased PPFD and enhanced plant growth. To align the solar spectrum with PPFD, the Bird Simple Spectral Model is utilized, offering different methods for PPFD calculation. Conversion factors from the solar energy spectrum to PPFD for daylight are approximated, aiding in precise measurements of light intensity available for photosynthesis (Franklin, 1998). Equation (2) is used to calculate the PPFD for different greenhouse coverings. Also, the photosynthetic photon flux, $\varphi$ ($\lambda$), which shows the number of photosynthetic photons reached to the plant, and PPFD are correlated as shown in Equation (3) (Safat Dipta et al., 2022).

$$PPFD = 4.57\times \int_{400}^{700} PAR(\lambda)\times S(\lambda)\times \tau(\lambda) d\lambda \quad (2)$$

$$PPFD = \int_{400}^{700} \frac{\phi(\lambda)}{N_A \times 10^{-6}} d\lambda \quad (3)$$

$PAR(\lambda)$ is the photosynthetically active radiation response at wavelength $\lambda$, $S(\lambda)$ is the solar spectral irradiance at wavelength $\lambda$, and $\tau(\lambda)$ is the spectral transmittance of the material at wavelength $\lambda$. $N_A$ is the Avagodro's number. Based on calculations, the photosynthetic photon flux, $\varphi$ ($\lambda$), is demonstrated in Fig. 11 for single-layer, double-layer, and PE-ATO4 greenhouse coverings. As is expected, utilizing ATO coating on the covering caused a little drop in photosynthetic photon flux, which was compensated by artificial lighting to not affect plant growth. The impact of this compensation by artificial lighting on lighting energy is comprehensively discussed in section 3.4.

Based on PPFD calculations, PPFD values of different greenhouse coverings are compared in Table 4.

**Table 4**
PPFD and PST values.

| Greenhouse covering | PPFD ($\frac{\mu mol}{m^2 s}$) | PPFD change relative to Single-layer PE (%) | PST | PST change relative to Single-layer PE (%) |
|---|---|---|---|---|
| Single-layer PE | 408.9 | - | 0.99 | - |
| Double-layer PE | 343.4 | −16.0% | 0.97 | −2.0% |
| PE-ATO4 | 357.0 | −12.7% | 1.73 | +74.7% |

#### 3.3.2. PAR-to-Solar-Transmittance (PST)

Exploring solar light quality's impact on plant photosynthesis, key pigments (carotenoid, chlorophyll *a*, and *b*) and the photosynthesis action spectrum (400–700 nm) is crucial. Plant pigments exhibit peak absorption in the blue and red bands, with lower absorption in the green band. Mecree curve (photosynthesis action spectrum) illustrates notable peaks at 450 nm (chlorophyll *b*) and 680 nm (chlorophyll) (Bugbee, 2016). A PAR-to-Solar-Transmittance (PST) value is defined to express the relationship between the relevant PAR region transmittance and the full spectrum solar transmittance and is calculated as follows:

$$PST = \frac{\tau_{PAR}}{\tau_S} \quad (4)$$

$$\tau_{PAR} = \frac{\int_{400}^{700} \tau(\lambda)\times PAR(\lambda)\times S(\lambda) d\lambda}{\int_{400}^{700} PAR(\lambda)\times S(\lambda) d\lambda} \quad (5)$$

$$\tau_s = \frac{\int_{400}^{2500} \tau(\lambda)\times S(\lambda) d\lambda}{\int_{400}^{2500} S(\lambda) d\lambda} \quad (6)$$

Where $\tau_s$ is the covering total solar transmittance, and $\tau_{PAR}$ is the covering solar transmittance in the PAR region. The calculated PST values for different greenhouse coverings are shown in Table 4.

As depicted in Table 4, the utilization of ATO nanoparticle coatings on PE films results in a significant rise in their PST values, almost 75% in

**Table 5**
Climate zones and corresponding summer and winter definitions. The weather dataset for each city is obtained from the EnergyPlus website (EnergyPlus, n.d.).

| Climate Zone | Representative City | Summer months (external)(low SHGC) | Winter months (internal)(high SHGC) |
|---|---|---|---|
| 1 (very hot) | Honolulu, HI | Jan–Dec | – |
| 2 (hot) | Tucson, AZ | Jan–Dec | – |
| 3 (warm) | El Paso, TX | Feb–Dec | Jan |
| 4 (mixed) | Alburquerque, NM | Mar–Nov | Dec–Feb |
| 5 (cool) | Denver, CO | Apr–Nov | Dec–Mar |
| 6 (cold) | Great Falls, MT | May–Oct | Nov–Apr |
| 7 (very cold) | International Falls, MN | May–Sep | Oct–Apr |
| 8 (Subarctic) | Fairbanks, AK | Jun–Aug | Sep–May |

comparison with the uncoated films. This improvement signifies that the ATO coatings enhanced the film's capacity to selectively filter solar heat while permitting a considerable transmission of PAR. This comparative assessment highlights that, in terms of PST values or spectral selectivity for solar heat control, PE films with four layers of ATO nanoparticles exhibited superior performance.

### 3.4. Energy savings of using PE-ATO4 coverings

The heating, cooling, lighting, and total (including heating, cooling, lighting, and fans operation) energy consumption of the greenhouse were calculated by applying different coverings on the greenhouse for eight US climate zones from very hot weather conditions (Zone 1) to Subarctic (Zone 8). Summer and winter seasons were defined individually for each climate zone based on our previous work (Anwar Jahid et al., 2022). The monthly energy consumption was calculated for each climate zone with both summer and winter conditions. Then, based on the energy consumption results, the best month to flip the covering was determined for each climate. The studied climate zones and their corresponding summer and winter months are presented in Table 5, which is upon the dominant HVAC mode of each month. Based on Tables 5, in very hot and hot climates (Zone 1 and Zone 2), summer includes all months of the year, meaning that the coating should be placed externally all the time. However, in colder climates like Zone 7 and Zone 8, summer includes just a few months of the year and coating should be placed internally most of the year.

Fig. 12 illustrates a set of energy simulation results of the greenhouse with different coverings (single-layer PE, double-layer PE, and PE-ATO4) in summer, winter, and whole year in various climate zones. In general, as expected, in the first three climate zones (1, 2, and 3), heating energy consumption is too little, and lighting mainly contributes to the total energy consumption. On the other hand, in the 5 remaining climate zones (4, 5, 6, 7, and 8) heating contribution goes up and becomes the major energy consumption in the greenhouse.

From the total energy consumption perspective, as the cooling and lighting energy was increased, using PE-ATO4 coverings increased the total energy consumption in the summer season rather than single-layer PE in all climate zones except Zone 5. But still using PE-ATO4 achieved less energy consumption than double-layer PE covering. The heating energy consumption in Zone 5 was relatively high in the summer months. Therefore, there was a trade-off between heating, cooling, and lighting energy consumption there, and ultimately, the total energy consumption in summer decreased. In winter, however, the total energy consumption was reduced in all climate zones by using PE-ATO4 coverings. As mentioned, employing PE-ATO4 coverings led to a reduction in heating energy, and heating energy usage constitutes the major energy consumption in winter months. The effect of PE-ATO4 on total energy consumption throughout the year was not the same in all climate zones. Table 6 shows the energy-saving percentage of the double-layer PE without ATO coating and with ATO coating (the baseline is the greenhouse with single-layer PE covering). As is shown in Table 6, deploying PE-ATO4 coverings resulted in more energy consumption in the hot climates (Zones 1 and 2) in the whole year than single-layer PE (energy savings are negative). In all other climates, applying PE-ATO4 resulted in energy savings throughout the year, and the colder the weather was, the more energy was saved. In comparison with single-layer PE, the total annual energy saving achieved by using PE-ATO4 covering reached 7199.67 GJ (from 15712.96 to 8513.29 GJ) in Zone 8. The highest total annual energy saving percentage occurred in Zone 7 with 48.3%. It means using PE-ATO4 coverings in very cold climates reduced the total annual energy consumption of the greenhouse to almost half. This percentage was near 20% for mixed climate zones and more than 40% for cold and subarctic climates. The third row of Table 6 demonstrates greenhouse energy performance improvement just caused by ATO coatings. It is noteworthy that in all climates, the total energy consumed by the greenhouse with PE-ATO4 coverings was less than the greenhouse with double-layer PE coverings. In comparison with double-layer PE without ATO coating, PE-ATO4 covering improved the greenhouse energy savings by 11.4% in Zone 7.

Following is a detailed analysis of the heating, cooling, and lighting energy consumption in the greenhouse.

- **Heating:** In all climate zones, the heating energy consumption is reduced by employing PE-ATO4 throughout the year, relative to single-layer and double-layer PE systems. In cold weather conditions, this reduction is much greater, and as is shown in Fig. 12, using PE-ATO4 obtains a huge reduction in heating energy consumption, which reaches about 7411 GJ (from 12532.77 to 5121.37 GJ) annual heating energy savings in Zone 8. The highest heating energy reduction percentage was for Zone 7 with nearly 70% annual heating energy savings.

ATO coatings significantly decreased the emissivity of the PE layer and as a result, the heat transfer coefficient (U-factor) of the covering decreased. In addition, based on the UV–Vis–NIR spectra, ATO coatings increase the absorption in the NIR region significantly. Therefore, the NIR light is absorbed by the ATO coating on the covering and reradiated inside in winter. This maintained the SHGC of the covering still at a relatively higher level although the overall transmittance of the PE-ATO4 is slightly reduced relative to the PE alone. It means that U-factor decreases and maintaining high SHGC by ATO coatings led to huge heating energy consumption reduction in the greenhouse in all climate zones. Fig. 13 shows the hourly heating energy consumption for 72 consecutive hours starting from 1:00 a.m., Dec. 19th to 12:00 a.m. Dec. 21st in Zone 7. Dec. 21st was the winter design day. The secondary vertical axis is the solar radiation rate per square meter reached by the greenhouse. Fig. 13 clearly shows daily heating energy savings by ATO coatings in the greenhouse. Based on the solar radiation demonstrated in Fig. 13, Dec. 19th was cloudy, and Dec. 20th and Dec. 21st were sunny days. But in both situations, PE-ATO4 covering had less heating energy use rather than single-layer and double-layer PE coverings. Thus, the sky's cloudiness did not affect the ATO coatings' performance.

- **Lighting:** Conversely, as shown in Fig. 12, the lighting energy consumption is increased by using PE-ATO4 in comparison with single and double-layer PE in all climate zones. This is because of that the

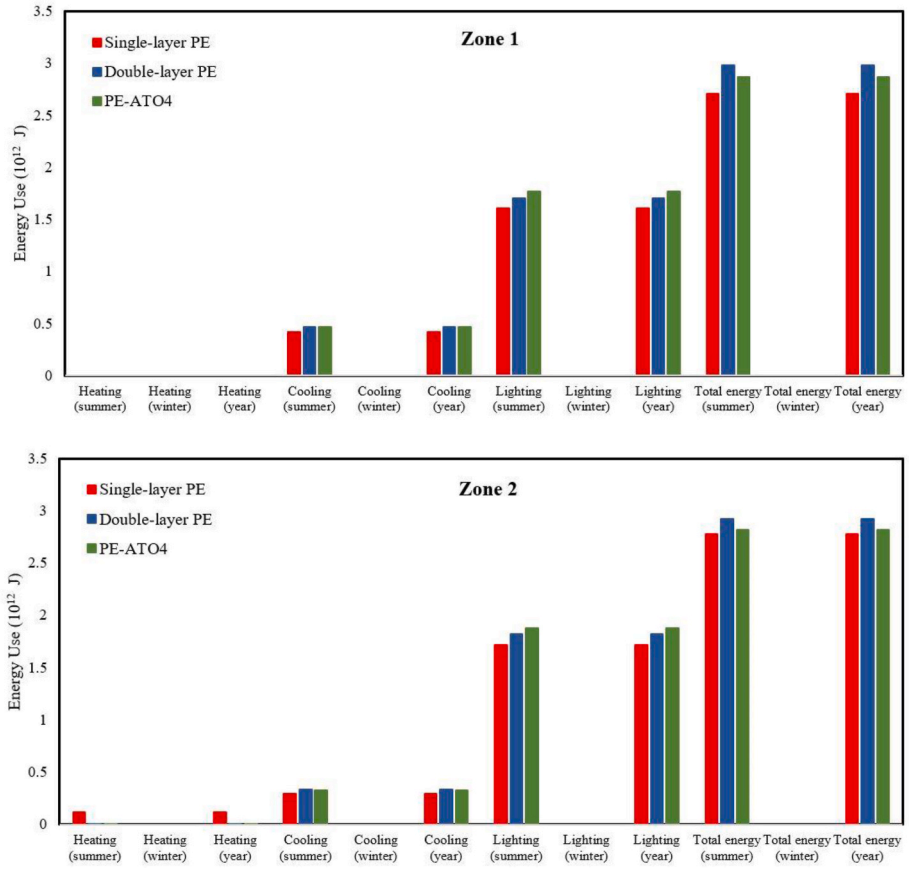


**Fig. 12.** The energy consumption of the greenhouse in various climate zones.

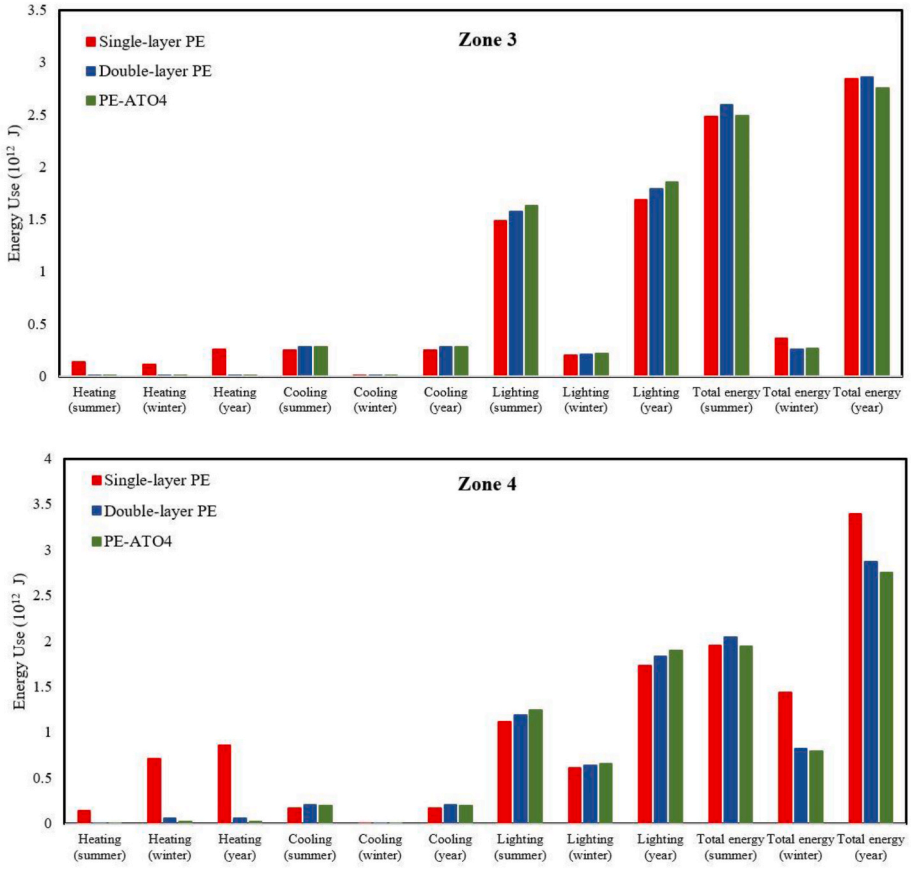


**Fig. 12.** (*continued*).

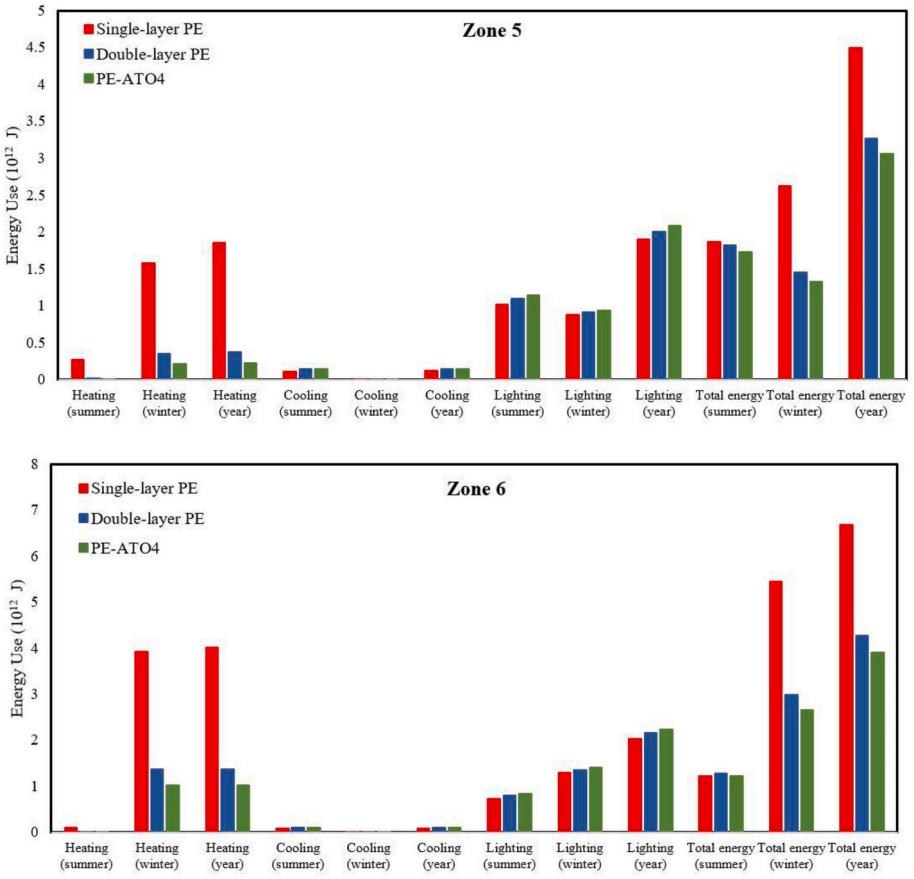


**Fig. 12.** (*continued*).

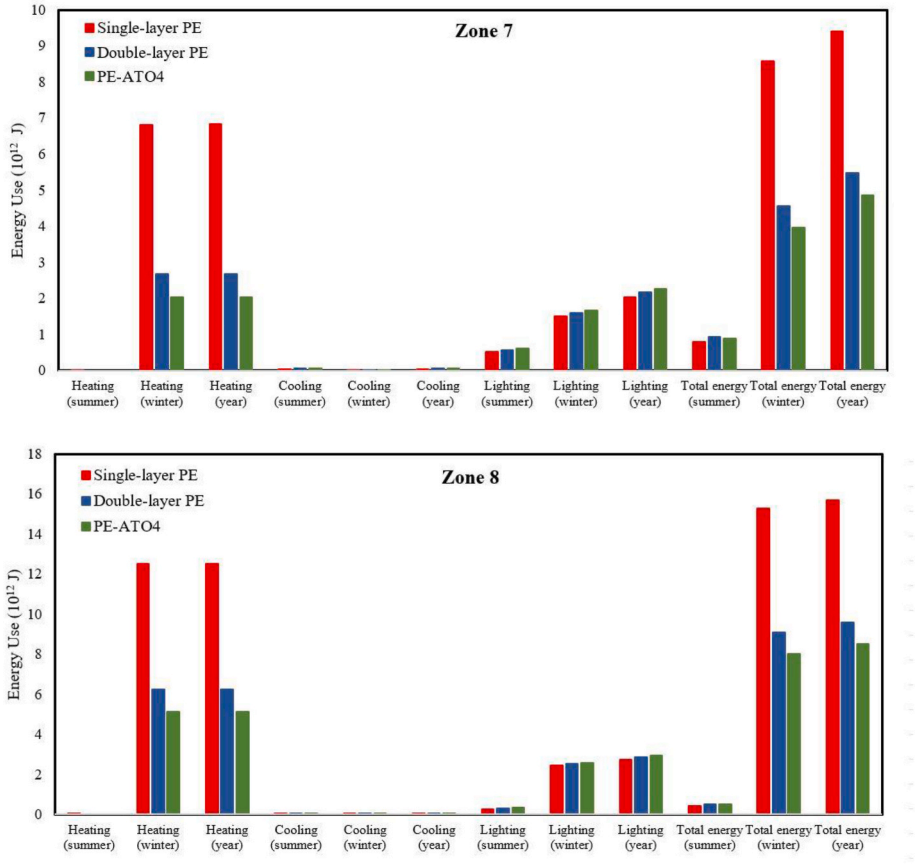


**Fig. 12.** (*continued*).

PAR transmittance of the PE-ATO4 covering is less than that of double-layer PE, and double-layer PE has less PAR transmittance than single-layer PE. Thus, more artificial lighting was needed to satisfy the required photosynthesis light in the greenhouse in such situations. The most lighting energy rise occurred in Zone 7, which increased from 2036 to 2270.11 GJ. It means approximately 11.5% of annual lighting energy consumption rose in this climate zone. In other climate zones, the increased lighting energy was less than 5%.

To better understand the features of lighting energy use, hourly data from July 19th to 21st is depicted in Fig. 14. The lighting system was programmed in the simulation to operate for 16 hours a day, turning off for the remaining 8 hours at night. This setup illustrates that lighting energy consumption is significantly influenced by solar radiation. Analyzing three different covering materials reveals notable differences in energy use, especially from 4 to 8 p.m., when reduced solar radiation increases the demand for electrical lighting. During these hours, the Photosynthetically Active Radiation (PAR) transmittance of the materials primarily dictates the electrical lighting needs. This also affects heat emissions from the lighting systems, which can be substantially impactful during the cooling season.

- **Cooling:** The extra artificial lighting discussed above causes the greenhouse to heat up and generates undesired heat in the greenhouse. Thus, the cooling system should remove this surplus heat produced by the lighting system and consume more energy to keep it at the desired temperature. Although the U-factor and the SHGC of the PE-ATO4 are less than single-layer PE's, based on Fig. 12, employing PE-ATO4 makes cooling energy consumption increase in all climate zones. However, this cooling energy rise was not enormous in comparison with heating energy reduction, and the most increase in cooling energy occurred in Zone 1 with only 47.15 GJ (from 422.66 to 469.81 GJ) in a year. In addition, using PE-ATO4 helped a little cooling energy reduction in comparison with double-layer PE in all climates.

Fig. 15 illustrates the hourly cooling energy consumption for Climate Zone 1 alongside solar radiation levels from July 19th to 21st. Generally, cooling energy consumption began to increase at sunrise and maintained its peak until sunset. During early morning hours with rapidly increased solar radiation and activated electrical lighting, the cooling energy reached its highest intensity for the day, and the difference in cooling energy between single-layer PE and PE-ATO4 was at its maximum. Interestingly, during nighttime, single-layer PE outperformed the other two covering systems. This enhanced performance was primarily due to its poorer insulation quality, which promotes natural cooling by taking advantage of the cooler outdoor air temperatures at night. Additionally, single-layer PE benefited from reduced heat emission, a result of decreased lighting energy use due to its higher PAR transmittance. Consequently, single-layer PE significantly reduced cooling energy consumption compared to the other covering options.

### *3.5. Optimizing energy savings through seasonal strategies on PE-ATO4 and single-layer PE*

As discussed above, applying ATO coatings on the greenhouse's covering reduced the energy consumption in winter months extensively, but it had a negative impact in summer months compared with single-layer PE. It means that to optimize energy consumption in the greenhouse; by starting the summer season (based on the definition of the

**Table 6**
Energy saving percentage by different coverings (the baseline is the greenhouse with a single-layer PE covering).

| | Zone 1 | Zone 2 | Zone 3 | Zone 4 | Zone 5 | Zone 6 | Zone 7 | Zone 8 |
|---|---|---|---|---|---|---|---|---|
| Double-layer PE w/o ATO | −9.9 | −5.2 | −0.5 | 15.5 | 27.1 | 36.0 | 41.6 | 38.9 |
| Double-layer PE w/ATO | −5.9 | −1.5 | 2.9 | 19.0 | 31.8 | 41.6 | 48.3 | 45.8 |
| Energy saving improvement just caused by ATO coating | 3.6 | 3.6 | 3.5 | 4.1 | 6.4 | 8.7 | 11.4 | 11.2 |

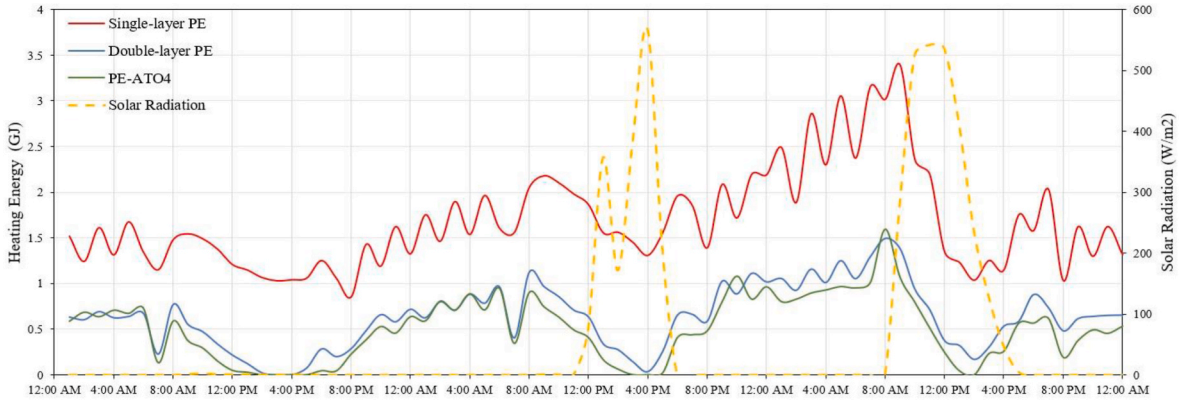


**Fig. 13.** Hourly heating energy consumption (from 1:00 a.m., Dec. 19th to 12:00 a.m. Dec. 21st in Zone 7).

summer in this study for each climate zone), the ATO-coated PE layer should be removed from the existing greenhouse structure and just single-layer PE being used in the summer. When the winter season starts, the coated PE layer should be added to the covering and the coating should be internal (winter mode). Overall, under such application modes combining single-layer PE and PE-ATO4, ATO coatings helped in energy savings throughout the year in all climate zones except very hot and hot climates (1 and 2). The only exception is in Zone 5 where PE-ATO4 applications in both summer and winter outperformed the performance of the combination mode. Fig. 16 shows the energy-saving percentages using such optimal combination mode (PE-ATO4) in winter and single-layer PE in summer (except for Zone 5) in comparison

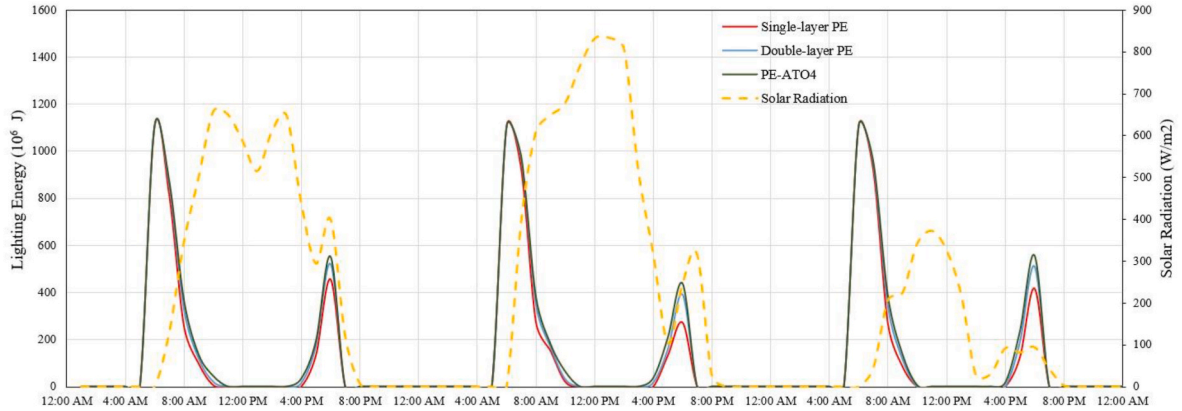


**Fig. 14.** Hourly lighting energy consumption (from 1:00 a.m., July 19th to 12:00 a.m. July 21st in Zone 1).

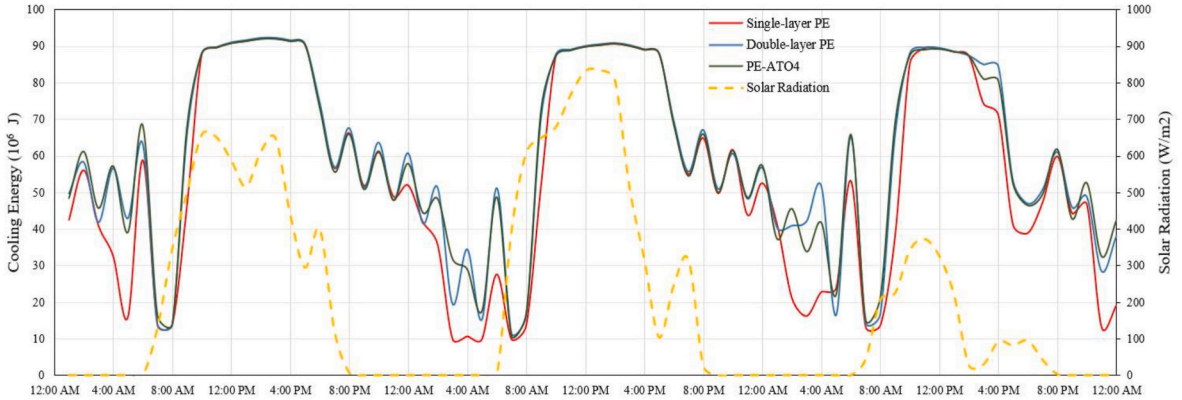


**Fig. 15.** Hourly cooling energy consumption (from 1:00 a.m., July 19th to 12:00 a.m. July 21st in Zone 1).

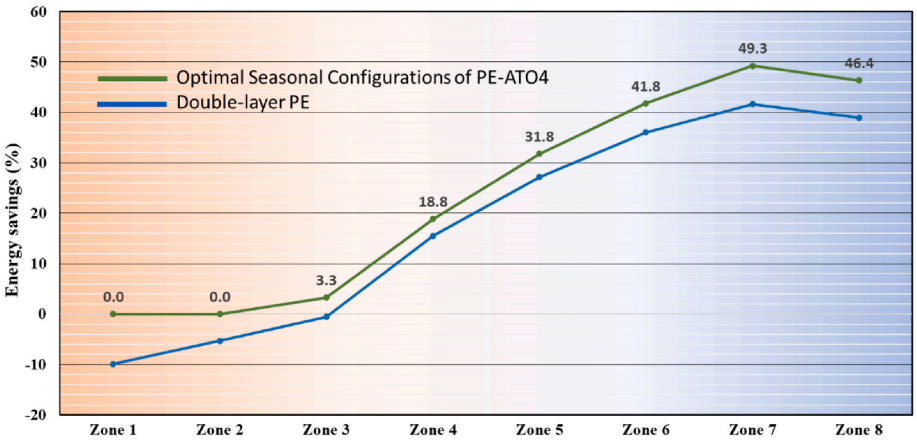


**Fig. 16.** Energy saving percentage relative to single-layer PE by using optimal seasonal setup of PE ATO4 and double-layer PE across different climatic zones.

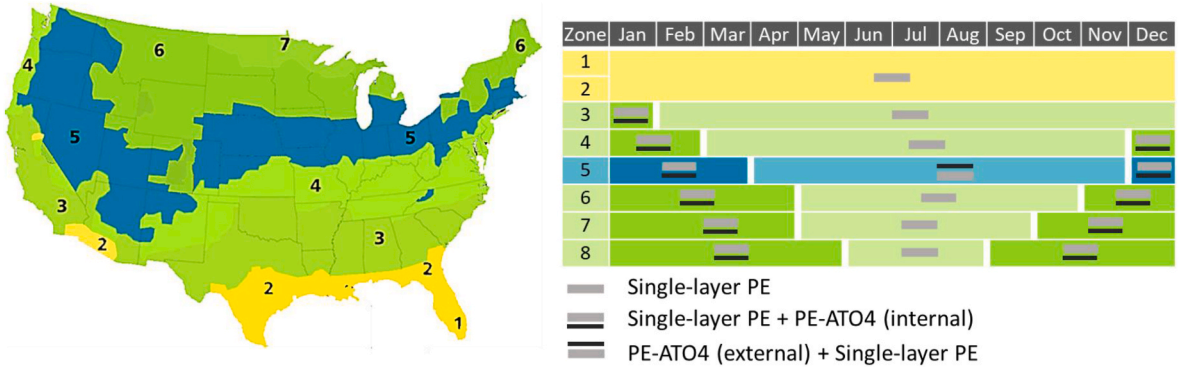


**Fig. 17.** Simplified guidelines of PE-ATO4 applications across different climatic zones.

with the single-layer PE (baseline).

As demonstrated in Fig. 16, in very hot and hot climates (zones 1 and 2) the best option is single-layer PE covering, and even using double-layer PE inversely impacts energy savings. In the warm climate (i.e. Zone 3), PE-ATO4 achieved a little, 3.32% energy saving throughout the year, but double-layer PE still had a negative impact. However, in mixed climate, Zone 4, PE-ATO4 facilitated nearly 20% energy savings, and in cool (5), cold (6), very cold (7), and subarctic (8) climates applying ATO coatings obtained huge yearly energy savings of approximately 29%, 42%, 49%, and 46%, respectively. Although the most energy saving occurred in Zone 8 with 7.2 TJ energy consumption reduction, the highest energy saving percentage, in comparison with single-layer PE, was for Zone 7 with 49% energy savings. Furthermore, in comparison with double-layer PE, PE-ATO4 covering was more effective and obtained more energy savings in all climate zones. Based upon the above analysis results, optimized seasonal strategies of using PE-ATO4 coverings can be achieved using a climate zone map (Burleyson, 2020), Fig. 17. By using Fig. 17, depending on the zone number of the city in which the greenhouse is located, the ATO-coated PE layer can be added during the specific months for operational energy saving purposes.

## 4. Conclusion

A new greenhouse covering coating based on photothermal plasmonic nanoparticles was introduced, and its potential energy savings in the greenhouse were investigated. Antimony tin oxide (ATO) nanoparticles were spin-coated on PE films and the uniform deposition was verified by various characterization methods. The optical and thermal properties of the ATO-coated PE films were measured. A greenhouse energy model was developed, and the energy simulation was executed for eight different US climate zones. The photosynthetically active radiation (PAR) transmittance of the ATO-coated covering was 0.746, and the PAR-to-Solar-Transmittance (PST) value of the covering raised about 75%. The energy performance of a greenhouse with the developed covering was compared with ones with single-layer polyethylene and double-layer polyethylene coverings. Based on the results, ATO nanocoating reduces total greenhouse energy consumption by 11.4%. In comparison with single-layer polyethylene covering, double-layer polyethylene covering with ATO coating reduces greenhouse's heating load by 70% and subsequently decreases the total greenhouse energy consumption up to 49% without compromising required photosynthesis active radiation. However, results showed that ATO coating increases greenhouse lighting and cooling energy consumption. As a result, applying ATO coating is effective in warm, mixed, cool, cold, very cold, and subarctic climates (six out of eight studied climate zones) and is not effective in very hot climates due to lighting and cooling energy consumption increase. This study shows photothermal plasmonic nanoparticles have great potential to be used as coating material to manipulate optical and thermal properties of greenhouse coverings to control heat transfer through greenhouse and reduce energy consumption in greenhouses without affecting plant growth.

## CRediT authorship contribution statement

**Mohammad Elmi:** Writing – original draft, Visualization, Validation, Software, Methodology, Investigation, Formal analysis. **Enhe Zhang:** Writing – original draft, Software, Resources, Formal analysis, Data curation. **Anwar Jahid:** Writing – original draft, Software, Resources, Data curation. **Julian Wang:** Writing – review & editing, Writing – original draft, Supervision, Project administration, Formal analysis, Conceptualization.

## Declaration of competing interest

The authors declare that they have no known competing financial interests or personal relationships that could have appeared to influence the work reported in this paper.

## Acknowledgements

We acknowledge the financial support provided by the National Science Foundation CMMI 2001207 and USDA Natural Resources Conservation Service NR203A750008G006.

## Data availability

Data will be made available on request.

## References

Abdel-Ghany, A.M., Al-Helal, I.M., Alzahrani, S.M., Alsadon, A.A., Ali, I.M., Elleithy, R. M., 2012. Covering materials incorporating radiation-preventing techniques to meet greenhouse cooling Challenges in arid regions: a review. Sci. World J. 1–11. https://doi.org/10.1100/2012/906360.

Al-Helal, I.M., Abdel-Ghany, A.M., 2011. Energy partition and conversion of solar and thermal radiation into sensible and latent heat in a greenhouse under arid conditions. Energy Build. 43, 1740–1747. https://doi.org/10.1016/j.enbuild.2011.03.017.

Anwar Jahid, M., Wang, J., Zhang, E., Duan, Q., Feng, Y., 2022. Energy savings potential of reversible photothermal windows with near infrared-selective plasmonic nanofilms. Energy Convers. Manag. 263, 115705. https://doi.org/10.1016/j.enconman.2022.115705.

Baglivo, C., Mazzeo, D., Panico, S., Bonuso, S., Matera, N., Congedo, P.M., Oliveti, G., 2020. Complete greenhouse dynamic simulation tool to assess the crop thermal well-being and energy needs. Appl. Therm. Eng. 179, 115698. https://doi.org/10.1016/j.applthermaleng.2020.115698.

Brækken, A., Sannan, S., Jerca, I.O., Bădulescu, L.A., 2023. Assessment of heating and cooling demands of a glass greenhouse in Bucharest, Romania. Therm. Sci. Eng. Prog. 41, 101830. https://doi.org/10.1016/j.tsep.2023.101830.

Bugbee, B., 2016. Toward an optimal spectral quality for plant growth and development: the importance of radiation capture. Acta Hortic. 1–12. https://doi.org/10.17660/ActaHortic.2016.1134.1.

Burleyson, C., 2020. 2012 IECC Climate Zones. https://doi.org/10.25584/data.2020-05.1197/1617637.

Chavan, S.G., Maier, C., Alagoz, Y., Filipe, J.C., Warren, C.R., Lin, H., Jia, B., Loik, M.E., Cazzonelli, C.I., Chen, Z.H., Ghannoum, O., Tissue, D.T., 2020. Light-limited photosynthesis under energy-saving film decreases eggplant yield. Food Energy Secur. 9. https://doi.org/10.1002/fes3.245.

Chaysaz, A., Seyedi, S.R.M., Motevali, A., 2019. Effects of different greenhouse coverings on energy parameters of a photovoltaic–thermal solar system. Sol. Energy 194, 519–529. https://doi.org/10.1016/j.solener.2019.11.003.

Chen, C., Kuang, Y., Hu, L., 2019. Challenges and Opportunities for solar Evaporation. Joule 3, 683–718. https://doi.org/10.1016/j.joule.2018.12.023.

Chen, S., Zhu, Y., Chen, Y., Liu, W., 2020. Usage strategy of phase change materials in plastic greenhouses, in hot summer and cold winter climate. Appl. Energy 277, 115416. https://doi.org/10.1016/j.apenergy.2020.115416.

Choab, N., Allouhi, A., Maakoul, A. El, Kousksou, T., Saadeddine, S., Jamil, A., 2021. Effect of greenhouse design parameters on the heating and cooling requirement of greenhouses in Moroccan climatic conditions. IEEE Access 9, 2986–3003. https://doi.org/10.1109/ACCESS.2020.3047851.

Cui, X., Ruan, Q., Zhuo, X., Xia, X., Hu, J., Fu, R., Li, Y., Wang, J., Xu, H., 2023. Photothermal nanomaterials: a powerful light-to-heat converter. Chem. Rev. 123, 6891–6952. https://doi.org/10.1021/acs.chemrev.3c00159.

Curcija, D.C., Zhu, L., Czarnecki, S., Mitchell, R.D., Kohler, C., Vidanovic, S.V., Huizenga, C., USDOE, 2015. Berkeley Lab WINDOW. https://doi.org/10.11578/dc.20210416.62.

Elmi, M., Wang, J., 2023. Solar-thermal conversion in Envelope materials for energy savings. In: Advanced Materials in Smart Building Skins for Sustainability. Springer International Publishing, Cham, pp. 113–127. https://doi.org/10.1007/978-3-031-09695-2_5.

EnergyPlus, n.d. EnergyPlus Weather Data [WWW Document]. URL https://energyplus.net/weather.

Feng, C., Yuan, G., Wang, R., Chen, X., Ma, F., Yang, H., Li, X., 2024. Performance study on a novel greenhouse cover structure with beam split and heat control function. Energy Convers. Manag. 301, 118077. https://doi.org/10.1016/j.enconman.2024.118077.

Franklin, J., 1998. In: Langhans, R.W., Tibbits, T.W. (Eds.), Plant Growth Chamber Handbook. (Iowa Agriculture and Home Economics Experiment Station Special Report No. 99 (SR-99) and North Central Regional Research Publication No. 340 .), vol. 138, pp. 743–750. https://doi.org/10.1111/j.1469-8137.1998.149-7.x viii+240 with 20 t. New Phytol., 21×27·5 cm.

Gislerød, H.R., Mortensen, L.M., Torre, S., Pettersen, H., Dueck, T., Sand, A., 2012. Light and energy SAVING IN MODERN greenhouse production. Acta Hortic. 85–97. https://doi.org/10.17660/ActaHortic.2012.956.7.

Hooshmandzade, N., Motevali, A., Reza Mousavi Seyedi, S., Biparva, P., 2021. Influence of single and hybrid water-based nanofluids on performance of microgrid photovoltaic/thermal system. Appl. Energy 304, 117769. https://doi.org/10.1016/j.apenergy.2021.117769.

Hosseini-Fashami, F., Motevali, A., Nabavi-Pelesaraei, A., Hashemi, S.J., Chau, K., 2019. Energy-Life cycle assessment on applying solar technologies for greenhouse strawberry production. Renew. Sustain. Energy Rev. 116, 109411. https://doi.org/10.1016/j.rser.2019.109411.

Hosseini, M., Shahverdian, M.H., Sayyaadi, H., Javadijam, R., 2024. Renewable energy supplying strategy for a greenhouse based on the water-energy-economy nexus. J. Clean. Prod. 457, 142388. https://doi.org/10.1016/j.jclepro.2024.142388.

Iddio, E., Wang, L., Thomas, Y., McMorrow, G., Denzer, A., 2020. Energy efficient operation and modeling for greenhouses: a literature review. Renew. Sustain. Energy Rev. 117, 109480. https://doi.org/10.1016/j.rser.2019.109480.

Indhu, A.R., Keerthana, L., Dharmalingam, G., 2023. Plasmonic nanotechnology for photothermal applications – an evaluation. Beilstein J. Nanotechnol. 14, 380–419. https://doi.org/10.3762/bjnano.14.33.

Jans-Singh, M., Ward, R., Choudhary, R., 2021. Co-simulating a greenhouse in a building to quantify co-benefits of different coupled configurations. J. Build. Perform. Simul. 14, 247–276. https://doi.org/10.1080/19401493.2021.1908426.

Katsoulas, N., Bari, A., Papaioannou, C., 2020. Plant responses to UV Blocking greenhouse covering materials: a review. Agronomy 10, 1021. https://doi.org/10.3390/agronomy10071021.

Katzin, D., Marcelis, L.F.M., van Mourik, S., 2021. Energy savings in greenhouses by transition from high-pressure sodium to LED lighting. Appl. Energy 281, 116019. https://doi.org/10.1016/j.apenergy.2020.116019.

Ke, X., Yoshida, H., Hikosaka, S., Goto, E., 2021. Optimization of photosynthetic photon flux density and light quality for increasing radiation-use efficiency in Dwarf Tomato under LED light at the Vegetative growth stage. Plants 11, 121. https://doi.org/10.3390/plants11010121.

Liu, G., Jiang, Y., Zhong, K., Yang, Y., Wang, Y., 2023. A time series model adapted to multiple environments for recirculating aquaculture systems. Aquaculture 567, 739284. https://doi.org/10.1016/j.aquaculture.2023.739284.

Ma, Q., Zhang, Y., Wu, G., Yang, Q., Yuan, Y., Cheng, R., Tong, Y., Fang, H., 2022. Photovoltaic/spectrum performance analysis of a multifunctional solid spectral splitting covering for passive solar greenhouse roof. Energy Convers. Manag. 251, 114955. https://doi.org/10.1016/j.enconman.2021.114955.

Muñoz-Liesa, J., Cuerva, E., Parada, F., Volk, D., Gassó-Domingo, S., Josa, A., Nemecek, T., 2022. Urban greenhouse covering materials: assessing environmental impacts and crop yields effects. Resour. Conserv. Recycl. 186, 106527. https://doi.org/10.1016/j.resconrec.2022.106527.

Nikolaou, G., Neocleous, D., Christou, A., Polycarpou, P., Kitta, E., Katsoulas, N., 2021. Energy and water related parameters in Tomato and Cucumber greenhouse crops in Semiarid Mediterranean regions. A review, Part II: Irrigation and Fertigation. Horticulturae 7, 548. https://doi.org/10.3390/horticulturae7120548.

Pacific Northwest National Laboratory (PNNL), 2023. 90.1 Prototype Building Models 90.1-2022 - Warehouse (Non-refrigerated).

Rabbi, B., Chen, Z.-H., Sethuvenkatraman, S., 2019. Protected Cropping in warm climates: a review of humidity control and cooling methods. Energies 12, 2737. https://doi.org/10.3390/en12142737.

Ravishankar, E., Booth, R.E., Hollingsworth, J.A., Ade, H., Sederoff, H., DeCarolis, J.F., O'Connor, B.T., 2022. Organic solar powered greenhouse performance optimization and global economic opportunity. Energy Environ. Sci. 15, 1659–1671. https://doi.org/10.1039/D1EE03474J.

Safat Dipta, S., Schoenlaub, J., Habibur Rahaman, M., Uddin, A., 2022. Estimating the potential for semitransparent organic solar cells in agrophotovoltaic greenhouses. Appl. Energy 328, 120208. https://doi.org/10.1016/j.apenergy.2022.120208.

Solovyev, A.A., Rabotkin, S.V., Kovsharov, N.F., 2015. Polymer films with multilayer low-E coatings. Mater. Sci. Semicond. Process. 38, 373–380. https://doi.org/10.1016/j.mssp.2015.02.051.

Xie, X., Liu, Y.-J., Hao, J.-J., Ju, L., Du, W.-C., Yang, H.-W., 2019. Feasibility study of a new solar greenhouse covering material. J. Quant. Spectrosc. Radiat. Transf. 224, 37–43. https://doi.org/10.1016/j.jqsrt.2018.11.004.

Xu, L., Wei, R., Xu, L., 2020. Optimal greenhouse lighting scheduling using canopy light distribution model: a simulation study on tomatoes. Light. Res. Technol. 52, 233–246. https://doi.org/10.1177/1477153519825995.

Zhang, E., Jahid, M.A., Wang, J., Wang, N., Duan, Q., 2023. Investigating impacts of condensation on thermal performance in greenhouse glazing and operational energy use for sustainable agriculture. Biosyst. Eng. 236, 287–301. https://doi.org/10.1016/j.biosystemseng.2023.11.005.